Synthesis and Cure Kinetics of Liquefied Wood/Phenol/Formaldehyde Resins

Hui Pan,[1,*] Todd F. Shupe,[1] Chung-Yun Hse[2]

[1]*School of Renewable Natural Resources, Louisiana State University AgCenter, Baton Rouge, Louisiana 70803*
[2]*Southern Research Station, U.S. Department of Agriculture Forest Service, Pineville, Louisiana 71360*

Received 25 July 2007; accepted 12 November 2007
DOI 10.1002/app.27756
Published online 29 January 2008 in Wiley InterScience (www.interscience.wiley.com).

ABSTRACT: Wood liquefaction was conducted at a 2/1 phenol/wood ratio in two different reactors: (1) an atmospheric three-necked flask reactor and (2) a sealed Parr reactor. The liquefied wood mixture (liquefied wood, unreacted phenol, and wood residue) was further condensed with formaldehyde under acidic conditions to synthesize two novolac-type liquefied wood/phenol/formaldehyde (LWPF) resins: LWPF1 (the atmospheric reactor) and LWPF2 (the sealed reactor). The LWPF1 resin had a higher solid content and higher molecular weight than the LWPF2 resin. The cure kinetic mechanisms of the LWPF resins were investigated with dynamic and isothermal differential scanning calorimetry (DSC). The isothermal DSC data indicated that the cure reactions of both resins followed an autocatalytic mechanism. The activation energies of the liquefied wood resins were close to that of a reported lignin–phenol–formaldehyde resin but were higher than that of a typical phenol formaldehyde resin. The two liquefied wood resins followed similar cure kinetics; however, the LWPF1 resin had a higher activation energy for rate constant k_1 and a lower activation energy for rate constant k_2 than LWPF2. © 2008 Wiley Periodicals, Inc. J Appl Polym Sci 108: 1837–1844, 2008

Key words: liquefied wood; phenol; novolac; DSC; kinetics (polym.)

INTRODUCTION

Interest in wood liquefaction as a novel technique of biomass utilization has received increased attention because of the constantly increasing demanding for fossil fuels as well as the environmentally friendly nature of liquefied wood products. Novolac-type liquefied wood resins can be prepared from liquefied wood and formaldehyde cocondensation with an acid catalyst. Alma et al.[1,2] and Lin et al.[3,4] investigated the effects of several variables, such as the phenol/formaldehyde molar ratio and catalyst concentration, on the physical properties of liquefied wood and mechanical properties of molding products from liquefied wood resins. It was found that the viscosity and flow temperature of the liquefied wood resins were higher than those of the commercial novolac resin. The mechanical properties of the molded products were comparable to those of the conventional novolac resin.

A comprehensive understanding of the cure kinetics of a liquefied wood resin is crucial to optimizing the bond strength of the resin and the mechanical properties of the liquefied wood resin products. An accurate cure kinetic model helps to predict the cure behavior of the resin for process design and control and thus optimize the cure process. Differential scanning calorimetry (DSC) has been widely used to elucidate key cure process parameters, such as the extent and rate of chemical conversion of the polymer cure reaction.[5] Two basic approaches are used in DSC techniques. One is the isothermal approach, in which a single cure temperature is used at a given cure cycle, and the other is the dynamic approach, in which the rate of heating is kept constant for a given cure cycle.

Many studies have investigated the cure kinetics of phenol–formaldehyde (PF) resins with dynamic and/or isothermal DSC. The Kissinger equation has been mostly used in the dynamic DSC method to calculate the activation energy of the cure reaction of PF resins.[6–8] The advantage of the dynamic DSC method is that it can provide extensive information on the cure reaction from only a single dynamic scan.[5] However, the method using the Kissinger model assumes an *n*th-order mechanism of the cure reaction. For the majority of thermoset cure reactions, dynamic DSC usually overestimates the kinetic parameters with respect to isothermal data.[9,10]

Lei et al.[11] summarized a detailed isothermal DSC method in their study of the cure kinetics of PF resins used for oriented strand board. Wang et al.[12]

This article (no. 06-40-0678) is published with the approval of the Director of the Louisiana Agricultural Experiment Station.

**Present address*: Calhoun Research Station, Louisiana State University Ag Center, Calhoun, Louisiana 71225.
Correspondence to: T. F. Shupe (tshupe@agcenter.lsu.edu).

compared the abilities of two model-free kinetic methods to model and predict the cure kinetics of commercial PF resoles. Because PF resins are the most commonly used adhesives in the wood composite industry, the effects of wood and wood–resin interactions on the cure kinetics of PF resins have been previously studied by DSC.[13–15] Lower cure temperatures and activation energies of the cure reaction of the PF resins were found in the presence of wood.[13,15] Some other factors, such as additives and the NaOH/phenol ratio during the synthesis process, also affected the cure kinetics of the PF resins.[9,16,17]

Lignin has been studied as a substitute for phenol in the synthesis of PF resins because its structure is similar to that of phenol. In addition, lignin is the wood component most susceptible to a liquefaction reaction.[18,19] The cure kinetics of lignin–phenol–formaldehyde (LPF) resins have also been studied, and the results show that LPF resins have higher activation energy than a typical PF resin.[10,20,21] However, no studies have been reported on the modeling of the cure kinetics of liquefied wood resins. Our previous study showed that wood liquefaction conducted in two different reactors resulted in different extents of reaction and might involve different liquefaction mechanisms.[19] As such, the objectives of this study were to synthesize liquefied wood resins from liquefied wood reacted in two different reactors, build cure kinetic models for the resins based on DSC analysis, and study the effect of liquefaction methods on the cure kinetics of the resins.

EXPERIMENTAL

Materials

Sawdust from the Chinese tallow tree (*Triadica sebifera* syn. *Sapium sebiferum*) was collected and oven-dried overnight at 80°C. The dried material was then ground to pass through a 20-mesh sieve. Industrial-grade phenol (90%) was used as the reagent solvent in the liquefaction. Hexamethylenetetramine (HMTA) and calcium hydroxide were used as a hardener and an accelerator, respectively, in the curing reaction. All other chemicals were reagent-grade.

Synthesis of the liquefied wood/phenol/formaldehyde (LWPF) cocondensed resin

The procedures for the synthesis of the LWPF resin are shown in Figure 1. Wood powder, phenol (phenol/wood = 2/1 w/w), and oxalic acid (5% w/w phenol) were premixed until a uniform mixture was obtained. The mixture was then transferred to the reactor. Two different reactors were used in the liquefaction stage: one was an atmospheric three-necked flask reactor (Kimble Glass Inc., Vineland, NJ) equipped with a condenser and a stirring stick, and the other was a sealed Parr reactor (Parr Instrument Co., Moline, IL). Both reactions were conducted at 180°C for 90 min.

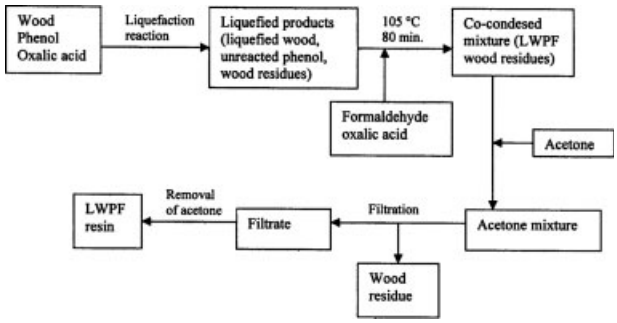

Figure 1 Flowchart of the synthesis of the LWPF resin.

The liquefied mixture was mixed with formaldehyde (36%) at a phenol/formaldehyde molar ratio of 1/0.8 (phenol was based on the initially charged amount) and additional oxalic acid (7 wt % phenol) and then refluxed in a 1-L Kimax reaction vessel (Vineland, NJ) under continued stirring at 105°C for 80 min. The resins synthesized from the liquefied wood reacted in the atmospheric flask and in the sealed Parr reactor were labeled LWPF1 and LWPF2, respectively. A small amount of the cocondensed mixture was dried under 105°C for 12 h after the synthesis and weighed to determine the solid content with the following equation:

$$\text{Solid content}(\%) = \frac{W_D}{W_O} \times 100 \quad (1)$$

where W_D is the weight of the dried resin and W_O is the weight of the original resin after synthesis. The cocondensed mixture was then diluted with acetone and vacuum-filtered to separate the wood residue and the dissolved resin. The wood residue was dried and weighed to determine the residue content with the following equation:

$$\text{Residue content}(\%) = \frac{W_R}{W_O} \times 100 \quad (2)$$

where W_R is the weight of the dried wood residue. Finally, the LWPF resin was obtained by pressure-reduced removal of the acetone.

Free phenol content measured by high-performance liquid chromatography (HPLC)

The amount of free phenol (i.e., unreacted phenol) in the liquefied wood mixture was measured on a PerkinElmer series 200 high-performance liquid chromatograph (Waltham, MA) with an Alltima HP C18 ODS column (250 × 4.6 mm) (Deerfield, IL). A meth-

TABLE I
Properties of the LWPF Resins

	Solid content (%)	Residue content (%)	Molecular weight		Free phenol (%)[c]	T_g (°C)[d]
			M_n[a]	M_w[b]		
LWPF1	55.62	17.96	1454.3	3476.6	63.02	64.02
LWPF2	37.69	11.22	1284.5	2692.9	51.12	50.15

[a] Number-average molecular weight.
[b] Weight-average molecular weight.
[c] Free phenol content in the liquefied wood.
[d] Glass-transition temperature.

anol/water (2/1 v/v) mixture was used as the mobile phase with the flow rate of 1.0 mL/min. The wavelength of the ultraviolet–visible detector in the HPLC series was set at 272 nm. A series of phenol solutions of known concentrations (0.06, 0.1, 0.15, 0.3, 0.5, and 0.7%) were used as the standard to calculate the amount of free phenol.

Gel permeation chromatography (GPC)

The molecular weight and molecular weight distribution of the LWPF resins were measured on a Waters Wyatt GPC system (Santa Barbara, CA) equipped with a differential refraction index detector. Two Jordi flash gel mixed bed columns (250 × 10 mm) (Santa Barbara, CA) were used in series. Tests were conducted at the ambient temperature with a tetrahydrofuran/methanol (90/10) mixture as the mobile phase at a flow rate of 1.0 mL/min. LWPF resin samples were dissolved in the same solvent as the mobile phase at a concentration of 5 mg/mL in solution. The amount of each sample injection was 100 μL. Polystyrene standards with a concentration of 1 mg/mL were used for calibration (the molecular weights were as follows: 393,400, 223,200, 111,400, 44,100, 31,600, 13,200, 3680, 2330, and 820).

Differential Scanning Calorimetry (DSC)

DSC measurements of the glass-transition temperature and the cure reaction of the LWPF resin were performed on a TA DSC-Q100 calorimeter. To measure the glass-transition temperature, about 10–15 mg of LWPF resin was put into an aluminum sample pan and sealed with a lid by crimping around the edge. An empty pan and a lid of the same type were used as a reference. The DSC temperature was programmed first from the ambient temperature to 250°C and back to 0°C at 20°C/min to eliminate the effect of water that might exist in the sample. The sample was then heated again to 250°C at the same rate.

To study the cure kinetics, the LWPF resin, HMTA, and calcium hydroxide were homogeneously mixed in a weight ratio of 1/0.2/0.25. A small amount (10–15 mg) of the sample was placed in a high-volume DSC sample pan that could withstand vapor pressures up to 10 MPa.

Two empty sample pans were used at the cure temperature to obtain a steady isothermal baseline. Four cure temperatures (120, 125, 130, and 135°C) were employed in the isothermal heating experiments for each LWPF resin. A continuous curve was obtained for each run, showing the rate of heat generated by the sample per gram as a function of time. The reaction was considered complete when the rate curve leveled off to the baseline. For each sample, after the first isothermal run, the sample was rapidly cooled in the DSC cell to 25°C, and the same isothermal run was started again. The curve used to calculate the heat of cure was obtained by subtraction of the curve of the second isothermal run from the first run. The total area under the exothermal curve, based on the extrapolated baseline at the end of the reaction, was considered the isothermal heat of cure at a given temperature.[11] Dynamic scans were also conducted with four heating rates (5, 10, 15, and 20°C/min) in a scanning temperature range from 25 to 200°C.

RESULTS AND DISCUSSION

Resin synthesis and properties

Some properties of the LWPF resin are summarized in Table I. Unlike a typical commercial phenolic resin, the solid content of the LWPF resin consists of the nonvolatile resin solid and the wood residue. Therefore, the content of the nonvolatile resin of the LWPF resin is the difference between the solid content and the residue content. It can be seen from Table I that the LWPF1 resin had higher nonvolatile resin and residue contents than the LWPF2 resin. An explanation of this result might be that the wood liquefaction conducted in a sealed system underwent a more thorough liquefaction reaction than that in the atmospheric system.[19] Table I also shows that liquefied wood which reacted in the sealed Parr reactor had a higher free phenol content than that in

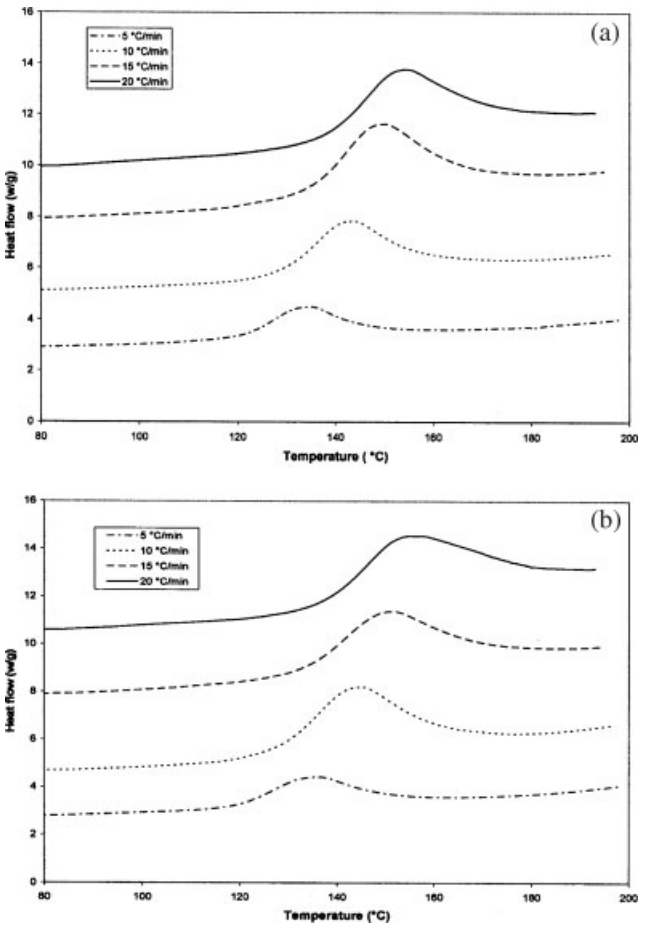

Figure 2 Dynamic DSC curves of (a) LWPF1 and (b) LWPF2.

the atmospheric three-necked flask. That is, more phenol reacted with the wood components, particularly lignin, and left less unreacted phenol in the sealed system than in the atmospheric system. Thus, the polymerization of the LWPF resin was retarded by either fewer functionality sites in the phenol or the steric hindrance of the lignin fragment combined onto the phenol.[10,20] The molecular weights of the LWPF resins also support this explanation to some extent. The LWPF2 resin had lower number-average and weight-average molecular weights than LWPF1. The glass-transition temperatures of the LWPF resins were consistent with the molecular weight results. In other words, the resin that had a higher average molecular weight presented a higher glass-transition temperature.

Dynamic DSC analysis

The dynamic DSC curves of the two LWPF resins at different heating rates are shown in Figure 2, and the results are listed in Table II. The onset and peak temperatures of both resins shifted to higher temperatures with an increased heating rate. The actual cure temperatures are independent of the heating rate; in other words, they are the temperatures at the heating rate of zero.[11] As listed in Table II, the cure reaction of the LWPF1 resin started at about 116°C and reached the highest cure rate around 129°C. Compared to LWPF1, LWPF2 had a lower onset temperature of 113°C and a little higher peak temperature of 130°C. The results show that the two LWPF resins had similar cure activities at the higher temperature of 130°C, whereas the LWPF2 resin was more active at lower temperatures than the LWPF1 resin.

Most other studies of the cure kinetics of LPF resins have used the dynamic DSC method. For comparison with LPF resins, the dynamic method developed by Kissinger[22] was also used in this experiment. The Kissinger equation is expressed as follows:

$$\ln\left(\frac{\phi}{T_p^2}\right) = -\frac{E}{R}\cdot\frac{1}{T_p} + \ln\left(\frac{RA}{E}\right) \tag{3}$$

where Φ is the heating rate (K/s), T_p is the peak temperature (K) at the given heating rate, A is the pre-exponential factor, R is the gas constant, and E is the activation energy. The activation energy can be obtained by linear regression from eq. (3). On the basis of this method, the activation energies of LWPF1 and LWPF2 were 96.55 and 97.54 kJ/mol, respectively. These values were higher than that of a typical PF resin reported by other researchers;[10,11] however, they were similar to that of an LPF resin.[20] This result may be due to the lower reactivity of the lignin fragments incorporated into the LWPF resin compared with that of phenol in conventional phenolic resins.[10,20]

Isothermal cure kinetics

In general, two kinetic models are used in the cure of thermosetting materials in terms of the mechanisms of their cure reaction: *n*th-order and autocata-

TABLE II
Cure Temperatures of Two Liquefied Wood Resins at Different Heating Rates

Heating rate (°C/min)	Onset temperature (°C)		Peak temperature (°C)	
	LWPF1	LWPF2	LWPF1	LWPF2
0[a]	115.8	113.3	128.7	129.9
5	121.0	118.6	134.2	135.2
10	127.1	125.6	142.5	143.8
15	133.5	131.2	148.8	150.0
20	137.6	136.4	153.5	154.4

[a] Extrapolated values from the intercepts of the plots of the onset temperatures and peak temperatures versus the heating rate.

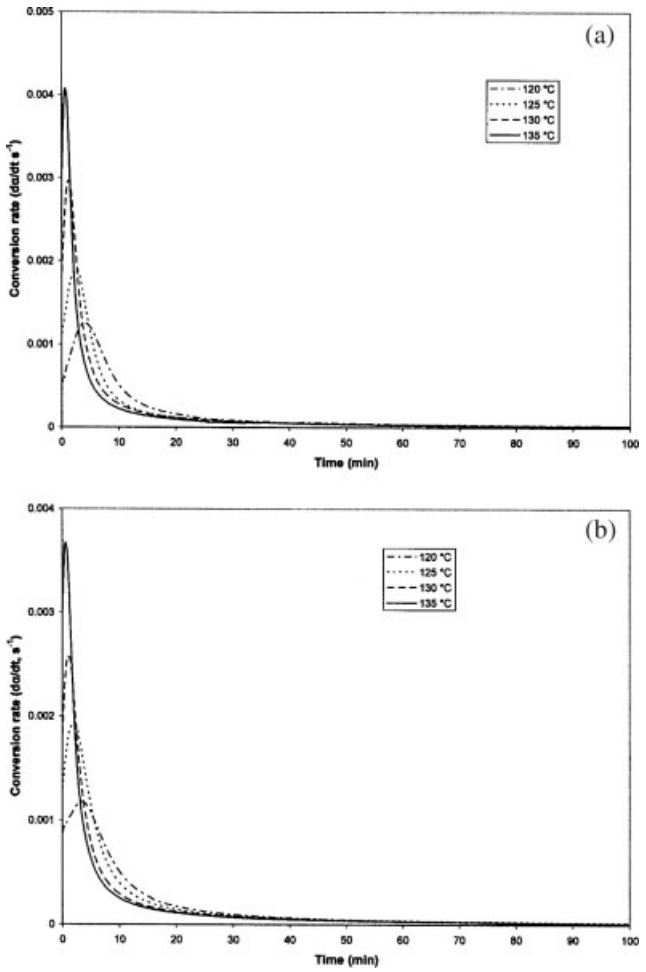

Figure 3 Conversion rate as a function of time at different isothermal temperatures for (a) LWPF1 and (b) LWPF2.

lytic. For thermosets that follow the *n*th-order kinetics, the conversion rate ($d\alpha/dt$) is proportional to the concentration of unreacted materials and can be expressed as follows:

$$\frac{d\alpha}{dt} = k(1-\alpha)^n \tag{4}$$

where α is the conversion of the reactant at time t and n is the reaction order. k is the temperature-dependent rate constant given by the Arrhenius equation:

$$k = A\exp(-E/RT) \tag{5}$$

where T is the absolute temperature. Autocatalytic thermoset cure reactions are the type in which one of the reaction products is also a catalyst for further reactions.[9] Thus, the reactions are characterized by an accelerating isothermal conversion rate and typically reach the maximum rate between 20 and 40% conversion.[9] The reaction rate is defined as follows:

$$\frac{d\alpha}{dt} = k'\alpha^m(1-\alpha)^n \tag{6}$$

where m and n are the reaction orders and k' is the rate constant, which is also given by the Arrhenius equation [eq. (5)]. To take into account that in the autocatalytic reactions the initial reaction rate is not zero, a generalized expression was proposed by Kamal[23] as follows:

$$\frac{d\alpha}{dt} = (k_1 + k_2\alpha^m)(1-\alpha)^n \tag{7}$$

where k_1 and k_2 are the rate constants. k_1 can be determined as the reaction rate at $t = 0$:

$$k_1 = \left(\frac{d\alpha}{dt}\right)_{t=0} \tag{8}$$

The basic assumption of the application of DSC for thermoset curing is that the measured heat flow (dH/dt) is proportional to the conversion rate ($d\alpha/dt$), and it has been proven to be a reasonably good

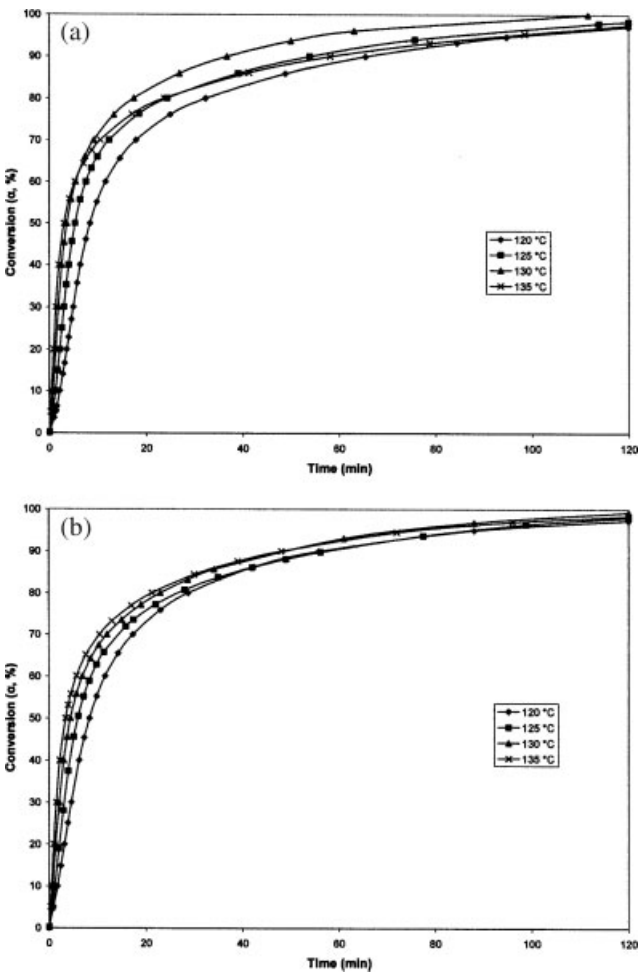

Figure 4 Conversion as a function of time at different isothermal temperatures for (a) LWPF1 and (b) LWPF2.

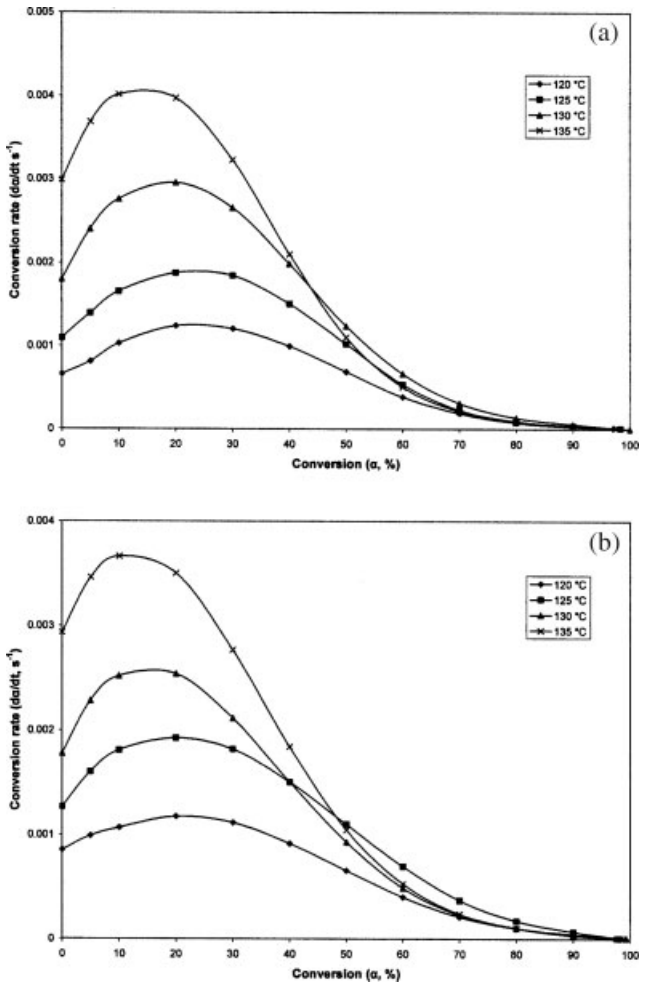

Figure 5 Conversion rate versus the conversion for (a) LWPF1 and (b) LWPF2.

assumption.[5] The rate of change in the conversion can therefore be defined as follows:

$$\frac{d\alpha}{dt} = \frac{dH/dt}{\Delta H_0} \tag{9}$$

where ΔH_0 is the total reaction heat associated with the cure process.

A series of isothermal DSC curves of the reaction rate as a function of time for the two liquefied wood resins are shown in Figure 3. It can be seen that with the increase in the cure temperature, the peak values of the reaction rate increased and shifted to shorter reaction times. The maximum conversion rate ($d\alpha/dt$) occurring at $t \neq 0$ suggests an autocatalytic cure kinetic mechanism for these two resins. By partial integration of the areas under the curves in Figure 3, the fractional conversion as a function of time was obtained and is plotted in Figure 4. Both of the liquefied wood resins reached about 70% conversion within 20 min at the testing temperatures. Generally, the higher the isothermal cure temperature was, the sooner the reaction reached the same percentage of conversion. However, the cure time was prolonged after the conversion reached 80% at the higher cure temperature of 135°C compared with that at 125 and 130°C. This phenomenon was possibly due to the onset of vitrification at higher cure temperatures. The mobility of the reaction groups could have been hindered, and the rate of conversion would then have been controlled by diffusion rather than chemical factors.[24,25]

Figure 5 shows the curves of the conversion rate as a function of conversion. It is clearly shown that the cure reaction of both liquefied wood resins follows an autocatalytic kinetic mechanism, with the maximum conversion rate in the 10–30% conversion region.

According to eq. (7) and with nonlinear regression,[11,25] the kinetic parameters of these two liquefied wood resins were calculated, and they are summarized in Table III. The average overall orders ($m + n$) of the cure reactions of LWPF1 and LWPF2 were 4.22 and 3.57, respectively. Rate constants k_1 and k_2 both obey the Arrhenius form [eq. (5)]. From linear regression, the associated activation energies (E_1 and E_2) and the pre-exponential factors were calculated, and they are listed in Table IV. The LWPF1 resin had a higher activation energy for k_1 and a lower activation energy for k_2. As shown in eq. (7), the term $k_2\alpha^m$ represents the influence of the reaction products on the conversion rate, and k_1 governs the early stage autocatalytic reaction.[5,25,26] As shown in Table I, LWPF1 had a higher average molecular weight than LWPF2. Because of the molecular mobility, the reactions between function groups on the molecules with low molecular weight seem easier than those on high-molecular-weight molecules. This might explain why LWPF1 had a higher initial activation energy than LWPF2 (Table IV). However, the

TABLE III
Isothermal Cure Kinetic Parameters of Two Liquefied Wood Resins

	LWPF1				LWPF2			
Temperature (°C)	k_1 (10^{-4} s^{-1})	k_2 (10^{-2} s^{-1})	n	m	k_1 (10^{-4} s^{-1})	k_2 (10^{-2} s^{-1})	n	m
120	6.62	1.15	3.03	1.20	8.54	0.59	2.53	1.01
125	10.93	1.71	3.19	1.14	12.69	0.86	2.42	0.90
130	17.99	1.78	3.09	0.95	17.81	0.87	2.87	0.74
135	29.84	1.81	3.49	0.81	29.36	1.13	3.04	0.74

TABLE IV
Activation Energies and Pre-Exponential Factors of Two Liquefied Wood Resins

Resin	E_1 (kJ/mol)	ln A_1	E_2 (kJ/mol)	ln A_2
LWPF1	133.76	33.61	37.61	7.15
LWPF2	107.70	25.87	52.82	11.08

LWPF1 resin had a lower activation energy for the subsequent reaction than LWPF2. This might result from more incorporated lignin fragment on LWPF2 than LWPF1, which might retard further polymerization (or condensation) of LWPF2.[10,20]

Thus, the kinetic equation for the liquefied wood resin LWPF1 is as follows:

$$\frac{d\alpha}{dt} = \left[3.94\times10^{14}\exp\left(-\frac{16087}{T}\right) + 1278\exp\left(-\frac{4523}{T}\right)\alpha^{1.02}\right] \times (1-\alpha)^{3.20} \quad (10)$$

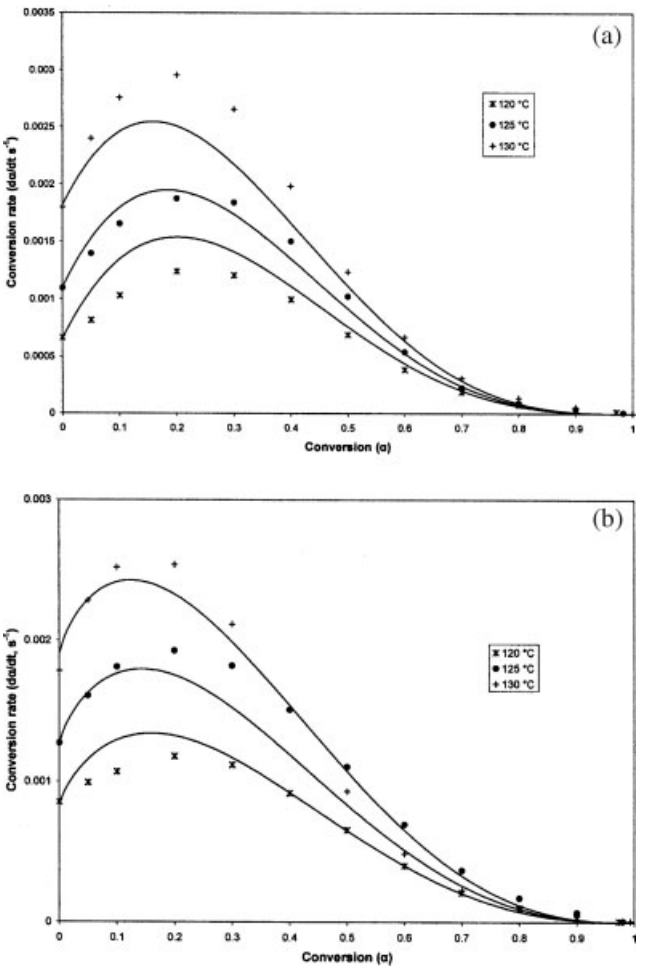

Figure 6 Comparison of the theoretical (lines) and experimental (symbols) conversion rates versus the conversion for (a) LWPF1 and (b) LWPF2.

The kinetic equation for the LWPF2 resin is

$$\frac{d\alpha}{dt} = \left[1.73\times10^{11}\exp\left(-\frac{12953}{T}\right) + 65190\exp\left(-\frac{6352}{T}\right)\alpha^{0.85}\right] \times (1-\alpha)^{2.72} \quad (11)$$

Figure 6 presents a comparison of the experimental data with the conversion rates obtained from the kinetic models [eqs. (10) and (11)]. It is clear that most predicted values agree with the experimental data.

CONCLUSIONS

Two LWPF resins were synthesized from liquefied wood reacted in atmospheric (LWPF1) and sealed (LWPF2) systems, and their cure kinetics were analyzed with DSC. The activation energies of LWPF1 and LWPF2 from the dynamic DSC method were 96.55 and 97.54 kJ/mol, respectively. These values were close to that of the LPF resin but higher than that of a typical PF resin. The onset cure temperatures of LWPF1 and LWPF2 were 115.81 and 128.66°C, respectively. The isothermal DSC results revealed autocatalytic cure mechanisms for both resins. The overall reaction orders for LWPF1 and LWPF2 were 4.22 and 3.57, respectively. The activation energies (E_1/E_2) for LWPF1 and LWPF2 were 133.76/37.61 and 107.70/52.82 kJ/mol, respectively. The kinetic results indicated that the two LWPF resins followed the same cure mechanism. However, the LWPF1 resin had a higher E_1 value but lower E_2 value than the LWPF2 resin.

The authors gratefully acknowledge Qinglin Wu for kindly providing the differential scanning calorimetry equipment and Yong Lei for his valuable discussion.

References

1. Alma, M. H.; Yoshioka, M.; Yao, Y.; Shiraishi, N. Mokuzai Gakkaishi 1995, 41, 1122.
2. Alma, M. H.; Yoshioka, M.; Yao, Y.; Shiraishi, N. Holzforschung 1996, 50, 85.
3. Lin, L.; Yoshioka, M.; Yao, Y.; Shiraishi, N. J Appl Polym Sci 1995, 58, 1297.
4. Lin, L.; Yoshioka, M.; Yao, Y.; Shiraishi, N. J Appl Polym Sci 1995, 55, 1563.
5. Boey, F. Y. C.; Qiang, W. Polymer 1999, 41, 2081.
6. Tsoul, C. T.; Yin, H. W.; Shiah, T. C. Taiwan Forestry Sci 2004, 19, 297.
7. He, G.; Yan, N. J Appl Polym Sci 2005, 95, 1368.
8. Sarbajna, R.; Ray, B. C. J Polym Mater 2004, 21, 71.
9. Park, B. D.; Riedl, B.; Hsu, E. W.; Shields, J. Polymer 1999, 40, 1689.
10. Alonso, M. V.; Oliet, M.; Perez, J. M.; Rodriguez, F.; Echevrria, J. Thermochim Acta 2004, 419, 161.
11. Lei, Y.; Wu, Q.; Lian, K. J Appl Polym Sci 2006, 100, 1642.
12. Wang, J.; Laborie, M. P.; Wolcott, M. P. Thermochim Acta 2005, 439, 68.

13. Pizzi, A.; Mtsweni, B.; Parsons, W. J Appl Polym Sci 1994, 52, 1847.
14. He, G.; Riedl, B. Wood Sci Technol 2004, 38, 69.
15. Lei, Y.; Wu, Q. J Appl Polym Sci 2006, 102, 3774.
16. Park, B. D.; Riedl, B.; Kim, Y. S.; So, W. T. J Appl Polym Sci 2002, 83, 1415.
17. Lei, Y.; Wu, Q. J Appl Polym Sci 2006, 101, 3886.
18. Pu, S.; Shiraishi, N. Mokuzai Gakkaishi 1993, 39, 446.
19. Pan, H.; Shupe, F. T.; Hse, C. Y. J Appl Polym Sci 2007, 105, 3739.
20. Barry, A. O.; Peng, W.; Riedl, B. Holzforschung 1993, 47, 247.
21. Simitzis, J.; Karagiannis, K.; Zoumpoulakis, L. Polym Int 1995, 38, 183.
22. Kissinger, H. E. Anal Chem 1957, 29, 1702.
23. Kamal, M. R. Polym Eng Sci 1974, 14, 23.
24. Opalicki, M.; Kenny, J. M.; Nicolais, L. J Appl Polym Sci 1996, 61, 1025.
25. Park, S. J.; Seo, M. K.; Lee, J. R. J Polym Sci Part A: Polym Chem 2000, 38, 2945.
26. Hseih, H. K.; Su, C. C.; Woo, E. M. Polymer 1998, 39, 2175.